Impact of Cloud Microphysics Parameter on 20th Century Warming Simulated in MRI-CGCM3

Tsuyoshi Koshiro, Hideaki Kawai, and Seiji Yukimoto

Meteorological Research Institute, Tsukuba, Japan

e-mail: tkoshiro@mri-jma.go.jp

1 Introduction

Recently, the treatment of clouds in global climate models has become more sophisticated. However, physics schemes related to clouds have a number of adjustable parameters; they are tuned to achieve the desired radiation balance for the best representation of the observed climate. Golaz et al. (2013) showed that variations in the autoconversion threshold radius ($r_{\rm crit}$), which controls the conversion of cloud water to rain, result in significantly different temperature evolutions over the 20th century in the CMIP5 GFDL-CM3 model. They suggested the presence of compensating model errors; the model characterized by the most plausible value of $r_{\rm crit}$ ($\sim$ 10 µm, derived from satellite observations; e.g., Suzuki et al., 2013) produced very unrealistic 20th century temperature evolutions.

In this study, we perform experiments similar to the aforementioned study to demonstrate the impact of the cloud microphysics parameter $r_{\rm crit}$ on the 20th century warming simulated by the CMIP5 MRI-CGCM3 model (Yukimoto et al., 2012). Golaz et al. (2013) regulated two additional parameters associated with cloud processes to keep the radiation balance within a desirable range; however, we vary only the value of $r_{\rm crit}$ to examine the climate response purely to this parameter. Moreover, we investigate the simulated cloud properties that may have caused the different temperature evolutions over the 20th century.

2 Method

We conducted two sets of CMIP5 MRI-CGCM3 historical simulations with alternative configurations of the $r_{\rm crit}$ value. We selected $r_{\rm crit}$ values smaller (5.0 µm, MRI-CGCM3w) and larger (10.0 µm, MRI-CGCM3c) than the default value used in MRI-CGCM3 (7.0 µm). The AMIP experiments (i.e., atmosphere-only experiments forced with observed sea surface temperatures) with these configurations confirmed that the top-of-atmosphere (TOA) net radiation values were within the acceptable range for the comparison of this study (Table 1). Initially, we performed preindustrial spin-up integrations for MRI-CGCM3w and MRI-CGCM3c, branching from the initial condition of the CMIP5 MRI-CGCM3 preindustrial control (piControl) simulation. These spin-up integrations were run for 100 years, so that the climate system could adjust to the modified $r_{\rm crit}$ over shorter time scales. The piControl simulations started from the final spin-up states. Subsequently, we created an ensemble of three historical members (1851–2005) starting every 30 years from the piControl simulations. Each piControl simulation was run for 215 years to cover the whole period of the historical ensemble.

Table 1: Summary of model configurations ($r_{\rm crit}$ values) with TOA net downward radiation for 1979–2008 obtained from the AMIP experiments.

	$r_{\rm crit}$ (µm)	TOA rad. (W m^{-2})
MRI-CGCM3w	5.0	−0.28
MRI-CGCM3 (CMIP5)	7.0	−1.04
MRI-CGCM3c	10.0	−3.52

3 Results

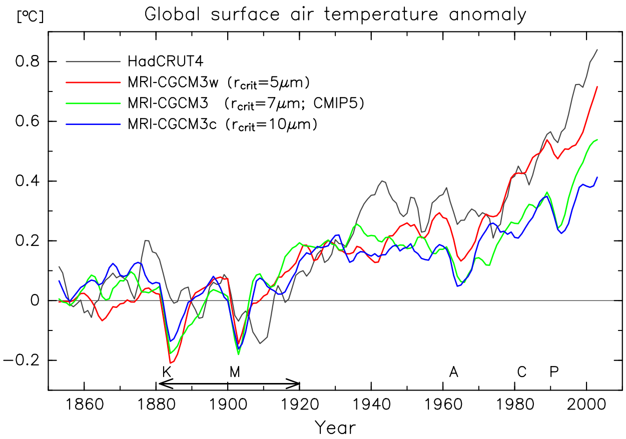

Fig. 1: Historical time series of global mean surface air temperature anomalies. Colored lines represent the CMIP5 MRI-CGCM3 model (green) and the two alternative configurations, MRI-CGCM3w (red) and MRI-CGCM3c (blue). Each line is a three-member ensemble average. Anomalies are calculated with respect to the period 1881–1920. Model drift is removed by subtracting the linear trend of the corresponding period in the piControl simulation from each ensemble member. Observations from HadCRUT4 (Morice et al., 2012) are also shown. A five-year running mean is applied to model results and observations. Letters above the horizontal axis represent major volcanic eruptions: Krakatoa (K), Santa María (M), Agung (A), El Chichón (C), and Pinatubo (P).

Figure 1 shows the temporal evolution of the global mean surface air temperature anomalies based on the CMIP5 MRI-CGCM3 historical simulations which considered different $r_{\rm crit}$ values. The standard CMIP5 MRI-CGCM3 underestimates the warming observed during the second half of the 20th century. MRI-CGCM3w more closely reflects the observations, except for the observed downward trend between the 1940s and 1970s. MRI-CGCM3c is generally colder than MRI-CGCM3, with indiscernible warming during the last period of the simulation. While the temperature from the HadCRUT4 observations increases by 0.59°C between 1881–1920 (preindustrial; denoted as PI) and 1981–2005 (present day; denoted as PD), the results of MRI-CGCM3w, MRI-CGCM3, and MRI-CGCM3c indicate temperature increases of 0.52°C, 0.36°C, and 0.31°C, respectively, for the same period. These results are consistent with Golaz et al. (2013), although the differences in the temperature evolutions among the configurations are smaller than their results.

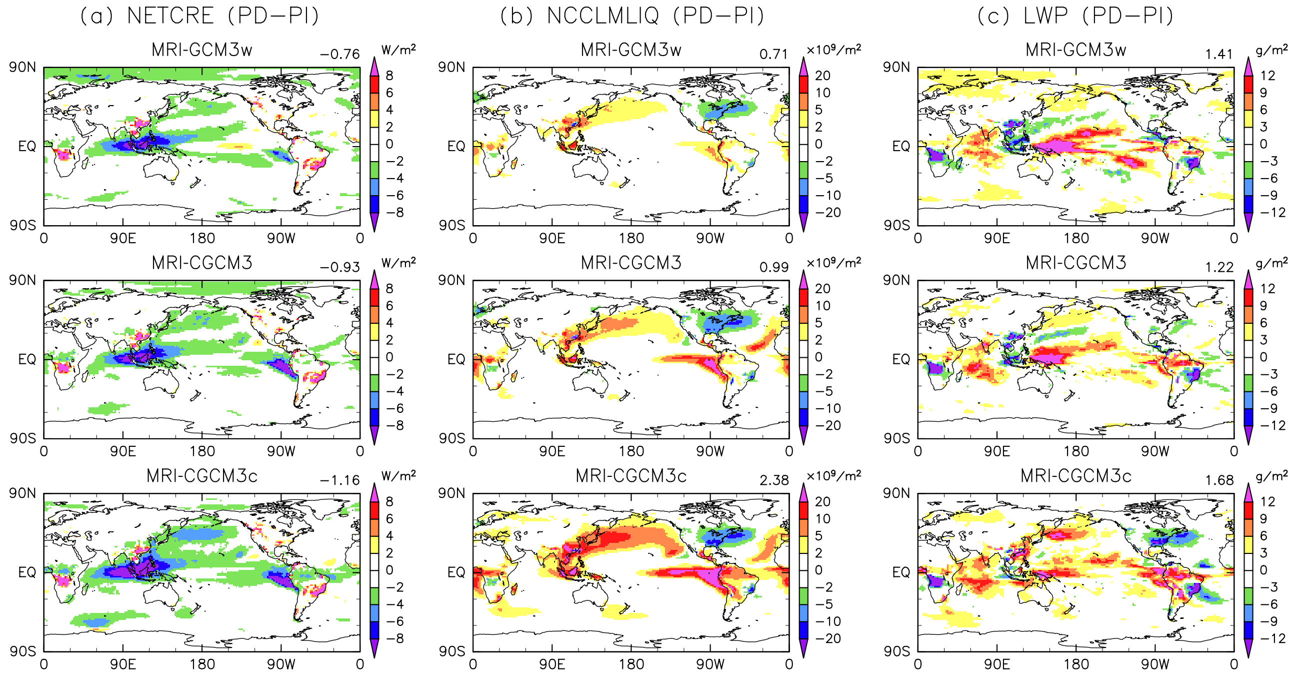

Fig. 2: PD–PI differences in annual and three-ensemble means of (a) net CRE (W m^{-2}; positive downwards), (b) column CDNC (10^9 m^{-2}), and (c) LWP (g m^{-2}) for MRI-CGCM3w (top), MRI-CGCM3 (middle), and MRI-CGCM3c (bottom). Global mean values are indicated at the top right of each panel.

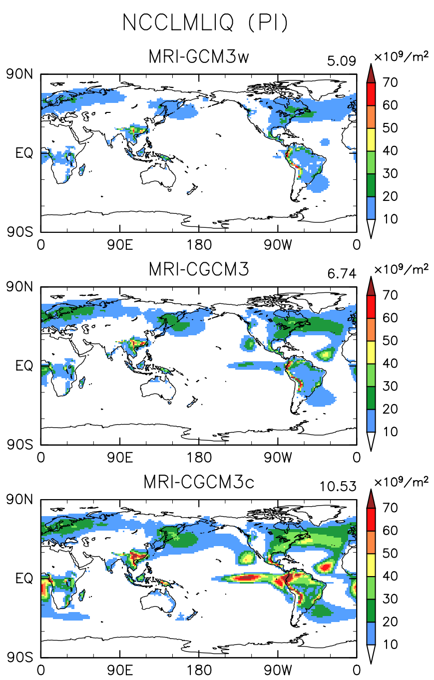

Fig. 3: Similar to Fig. 2b, but for PI annual and three-ensemble means.

Figure 2 displays the PD–PI differences in cloud properties for the three sets of the historical simulations. Figure 2a indicates that the differences between 20th century temperature evolutions are due to the net cloud radiative effect (CRE); the stronger the cloud radiative cooling (caused by shortwave solar reflection; not shown), the more underestimated the 20th century warming. The global mean values of the PD–PI difference in the net CRE are −0.76 W m^{-2}, −0.93 W m^{-2}, and −1.16 W m^{-2} in the case of MRI-CGCM3w, MRI-CGCM3, and MRI-CGCM3c, respectively. The absolute values of the negative net CRE and their variations among the configurations are large in the tropical eastern Pacific, the midlatitude North Pacific, and the western Maritime Continent.

As shown in Fig. 2b, these maxima are related to the column cloud droplet number concentration (CDNC). Notably, the differences in column CDNC among the configurations are largely derived from the baseline values of column CDNC under PI condition (Fig. 3); these differences grow further under PD conditions, due to the indirect effect of anthropogenic aerosols. The negative net CRE maxima over the subtropical North Pacific are more closely related to the liquid water path (LWP) than to the column CDNC; however, their differences among the configurations are not systematically clear (Fig. 2c). The baseline values of LWP (not shown) are comparable for different configurations.

Considering the baseline values shown in Fig. 3, our results are in contrast to the simple expectation that an increase in r_{crit} would lead to an increase in LWP, but would not significantly affect the CDNC. Further analysis is required to understand the behavior of cloud-to-rain conversion processes in MRI-CGCM3 for different r_{crit} values.

Acknowledgments

This work was supported in part by the Integrated Research Program for Advancing Climate Models (TOUGOU) Grant Number JPMXD0717935561 from the Japanese Ministry of Education, Culture, Sports, Science and Technology (MEXT), the Japan Aerospace Exploration Agency (JAXA) 2nd Research Announcement on the Earth Observations, the Environment Research and Technology Development Fund (2-2003) of the Environmental Restoration and Conservation Agency (ERCA) of Japan, and the Japan Society for the Promotion of Science (JSPS) KAKENHI Grant Numbers JP18H03363, JP19K03977.

References

Golaz, J.-C., L. W. Horowitz, and H. Levy II, 2013: Cloud tuning in a coupled climate model: Impact on 20th century warming. *Geophys. Res. Lett.*, **40**, 2246–2251, doi:10.1002/grl.50232.

Morice, C. P., and Coauthors, 2012: Quantifying uncertainties in global and regional temperature change using an ensemble of observational estimates: The HadCRUT4 data set. *J. Geophys. Res.*, **117**, D08101, doi:10.1029/2011JD017187.

Suzuki, K., J.-C. Golaz, and G. L. Stephens, 2013: Evaluating cloud tuning in a climate model with satellite observations. *Geophys. Res. Lett.*, **40**, 4464–4468, doi:10.1002/grl.50874.

Yukimoto, S., and Coauthors, 2012: A new global climate model of the Meteorological Research Institute: MRI-CGCM3 —Model description and basic performance—. *J. Meteor. Soc. Japan*, **90A**, 23–64, doi:10.2151/jmsj.2012-A02.